Incorporation of the Unusual Cα-Fluoroalkylamino Acids into Cyclopeptides: Synthesis of Arginine−Glycine−Aspartate (RGD) Analogues and Study of Their Conformational and Biological Behavior

Alma Dal Pozzo,*,† Minghong Ni,† Laura Muzi,† Roberto de Castiglione,† Rosanna Mondelli,‡ Stefania Mazzini,‡ Sergio Penco,§ Claudio Pisano,§ Massimo Castorina,§ and Giuseppe Giannini§

Istituto di Ricerche Chimiche e Biochimiche G. Ronzoni, Via G. Colombo 81, 20133 Milano, Italy, Dipartimento di Scienze Molecolari Agroalimentari, Università di Milano, Via Celoria 2, 20133 Milano, Italy, and Research and Development, Sigma-Tau, Pomezia, Roma, Italy

Received November 11, 2005

A series of six arginine−glycine−aspartate (RGD) cyclopeptide analogues containing a Cα-di- or trifluoromethylamino acid (α-Dfm or α-TfmAaa) at different positions of the ring were synthesized. All peptides were obtained in two diastereomeric forms, which were separated by HPLC. In vitro biological tests of the new cyclopeptides **P** were carried out in comparison with their corresponding cyclopeptides **R** lacking the α-fluoromethyl group. Five out of the six compounds **P-I** (containing (*S*)-α-Tfm-Aaa) showed activities in the nanomolar range, while the **P-II** compounds (containing (*R*)-α-Tfm-Aaa) were much less active or totally inactive. Only cyclo[RGDf-(*S*)-αTfmV] (**P1-I**) was found to be significantly more active than its model compound cyclo(RGDfV) (**R1**). The three-dimensional structure in water and DMSO was determined by NMR techniques and molecular dynamics (MD) calculations, but it was not possible to highlight significant differences in the backbone conformation of the peptides examined. Significant interproton distances, derived from nuclear Overhauser effect (NOE) experiments, were used to determine the absolute configuration of the side chains.

Introduction

On the basis of the observation that fluorinated analogues of naturally occurring compounds often exhibit unique physiological activities,[1] there has been increasing interest in fluorine-containing amino acids, and the relative chemistry is a developing area of interdisciplinary interest.[2,3] In the search for new unusual building blocks to be introduced into peptides and proteins with the purpose of modifying their physicochemical properties, Cα-fluoroalkylamino acids (FAaa) are particularly promising because they could greatly influence the bioavailability by improving the enzymatic stability and enhancing the lipophilicity that promotes permeability through the body barriers. FAaa share with other α,α-dialkylated amino acids the possibility of inducing secondary structures such as helices and β-turns, and additionally, their fluoroalkyl group is capable of participating in hydrogen bonding or of acting as a coordinative site in metal complexes[2] because of the availability of the nonbonding electron pairs; therefore, when strategically positioned in biologically active peptides, they could impart unpredictable properties, changing their activity and selectivity. As a consequence, such compounds can find potential applications in the biomedical field.

However, systematic investigations into structural and biological properties of FAaa have been impaired by the great synthetic difficulty of introducing these building blocks into peptides, and application of β-fluorine containing amino acids in peptide design is still in the early stages of development. In practice, incorporation of Cα-fluoroalkylated amino acids into peptides presents serious limitations because of the change of polarity of the functional groups and bonds in the vicinity of fluorine atom.[4] They were easily introduced by us and others at the N-terminus of some peptides,[5−8] but the problem of chain elongation by derivatization of the amino group is not feasible by common methods known to peptide chemistry, except for the least bulky α-TfmAla (Tfm = trifluoromethyl). Carboxy activation via chloride, in the presence of strong base, was successful in forming the amide bond but to the detriment of the acylating amino acid, which resulted in total racemization; thus, this drastic reaction is limited to substrates where epimerization is not possible.[6,9]

With the aim of verifying the assumption about the structural and biological effects of Cα-di-and trifluoromethylamino acids (α-Dfm and TfmAaa), we sought to incorporate them at different positions of well-known peptides like the arginine−glycine−aspartate (RGD) analogues, exhaustively studied by Kessler et al., as integrin inhibitors.[10−15] Integrins are a family of membrane adhesion receptors, which play an important role in angiogenesis and recognize proteins of the extracellular matrix through the amino acid sequence Arg-Gly-Asp. In the past decade, this universal recognition site became the basis for the development of a variety of potent and selective antagonists. In particular, the Kessler group designed and synthesized a series of cyclic peptides containing the RGD in an ideal conformation to exhibit the maximal affinity and selectivity toward α_v integrins, obtaining a bioactive compound that is being examined in clinical trials.[16]

We reasoned that these RGD analogues might represent suitable models for the purpose of studying the effects of the introduction of a β-fluorine substituted Aaa on the secondary structure and bioavailability.

Here, we report on the succeessful synthesis of RGD analogues containing α-Dfm or TfmAaa (in both diastereomeric forms) in different positions of the ring, whose structures are shown in Figure 1. In vitro biological tests and conformational

* To whom correspondence should be addressed. Phone: +39-02-70600223. Fax: +39-02-7064161. E-mail: dalpozzo@ronzoni.it.
† Istituto di Ricerche Chimiche e Biochimiche G. Ronzoni.
‡ Università di Milano.
§ Sigma-Tau.

10.1021/jm0511334 CCC: $33.50
Published on Web 02/09/2006

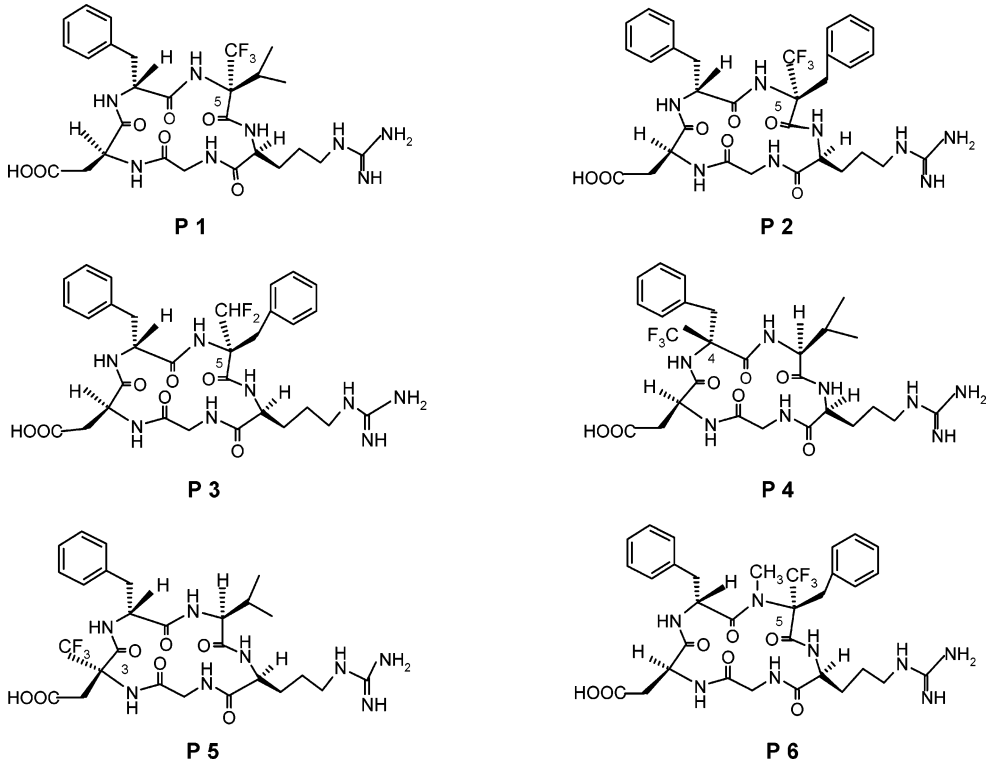

Figure 1. Structure of cyclopeptides containing C^{α}-fluoromethylamino acids, in their active *S* configuration.

Scheme 1. Synthesis of α-Dfm-amino Acid Ester

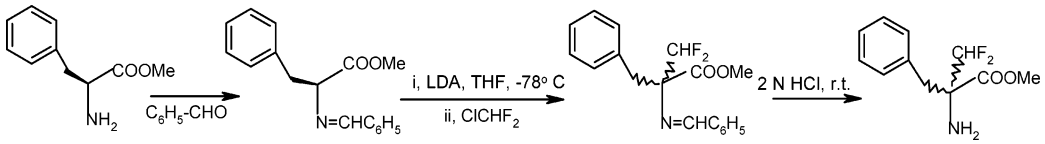

Scheme 2. Synthesis of *N*-Cbz-α-Tfm-amino Acid Esters

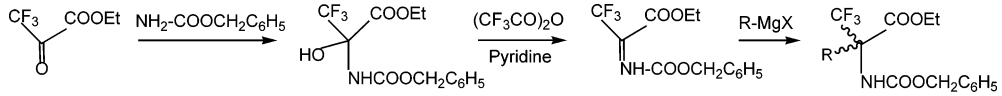

studies were performed in comparison with the model cyclopeptides lacking the α-fluoroalkylamino acid.

Results and Discussion

Chemistry. The synthesis of the *β*-fluorine containing amino acids was initially undertaken following methods described in the literature. The synthesis of the α-DfmAaa ester[17] proceeds via regioselective alkylation with chlorodifluoromethane of the Schiff base ester, readily available from the parent α-amino acid ester, according to Scheme 1. For the synthesis of α-TfmAaa esters,[18] trifluoropyruvate serves as an excellent intermediate for preparing the imine as the substrate to introduce the desired amino acid side chain, according to Scheme 2. *N*-Me-α-TfmPhe was introduced into the cyclic peptide in the form of its Leuch's anhydride, according to Scheme 3.[19]

The key step in the synthesis of the cyclopeptides is the formation of the amide bond between the α-fluoroalkyl building block and the preceding amino acid. This was achieved by exploiting a new coupling method recently developed in our laboratories. *N*-Phthaloylamino acid bromides were the acylating agents of choice for the synthesis of the cyclopeptides **P1**−**P4**. They were prepared in situ by the brominating reagent 1-bromo-*N*,*N*-2-trimethyl-1,1-propenylamine (bromoenamine) and immediately added to the amino acid ester to be acylated, in the

Scheme 3. Synthesis of *N*-Me-α-Tfm-Phe-carboxyanhydride

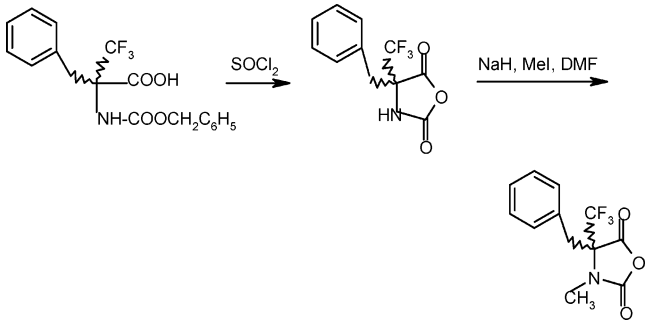

presence of collidine, following the procedure already described.[20] In the case of **P6**, containing *N*-Me-α-TfmPhe, which is extremely hindered, *N*-phthaloyl bromide failed to afford the coupling, and it was necessary to use the corresponding azidocarboxylic acid bromide because of its smaller size.[21−23] (Nevertheless, even with the use of this second procedure, it was not possible to introduce the still more hindered *N*-Me-α-TfmVal with reasonable yields.) The synthesis of **P5** represents an exception because the coupling between Gly and α-TfmAsp was achieved via Pht-Gly-Cl in the presence of TEA; in fact, with Gly as the acylating agent, there was no racemization problem.

Scheme 4. Synthesis of **P1-I** and **P1-II**, c[Arg-Gly-Asp-D-Phe-(*S* or *R*)-α-TfmVal][a]

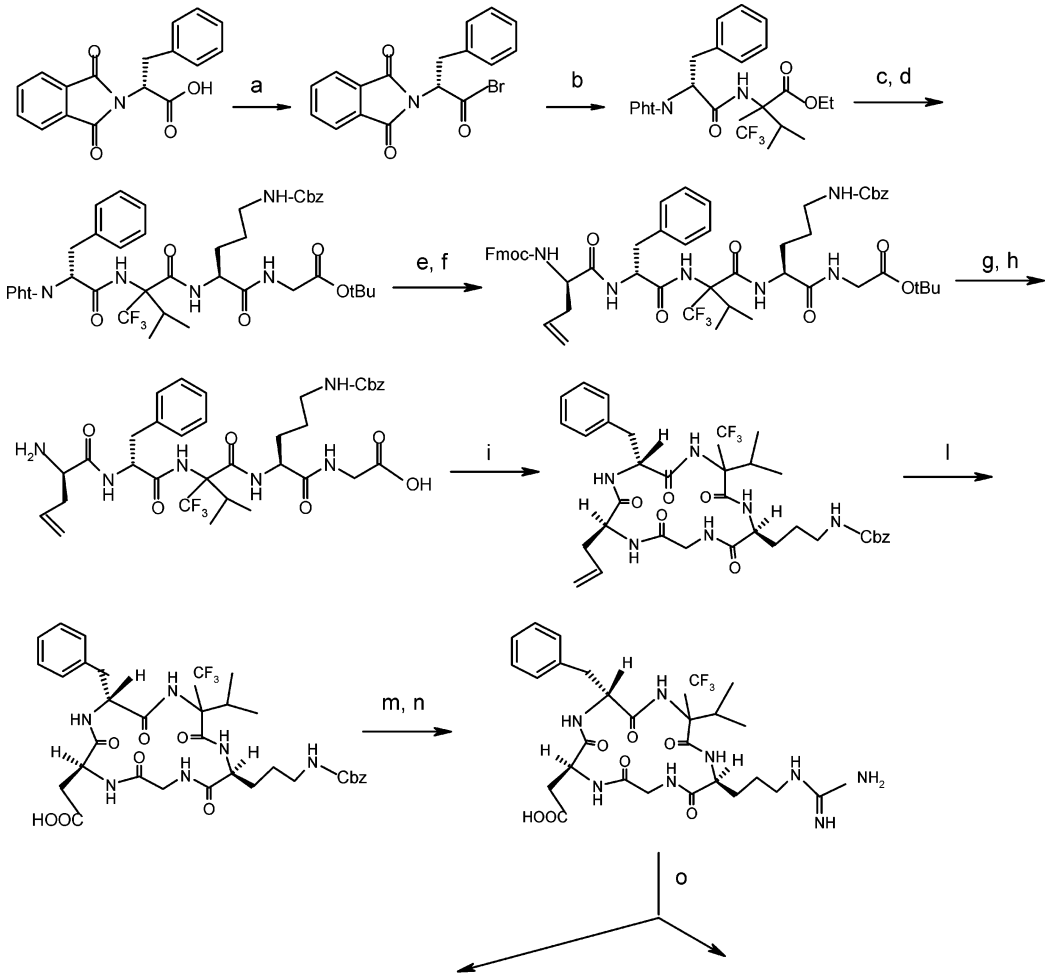

[a] Reagents and conditions: (a) bromoenamine, 1.2 equiv, DCM, argon, 10 min; (b) 0.2 equiv of HCl·α-TfmVal-OEt, DCM, 0 °C → room temp, 3 h; (c) 5 equiv of BBr_3, DCM, reflux, 4 h; (d) 2 equiv of H-Orn(Cbz)-Gly-OtBu, CH_3CN, 1.4 equiv of HATU, 2,8 equiv of DIEA, 1 h; (e) 1.5 equiv of $NH_2-NH_2 \cdot H_2O$, EtOH, reflux, 1.5 h; (f) 1 equiv of Fmoc-AllylGly-OH, 1 equiv of HOBT, 1 equiv of TBTU, 2 equiv of DIEA, CH_3CN, 1 h; (g) 10 equiv of piperidine, DCM, room temp, 2 h; (h) TFA/DCM 1:1, 1 h; (i) 10^{-3} M CH_3CN, 3 equiv of HOBT, 3 equiv of TBTU, 1% DIEA, 15 min; (l) 10:0.7 acetone/3 N H_2SO_4, 6 equiv of $KMnO_4$ aqueous solution, 0 °C → room temp, 1 night; (m) 10:1 MeOH/DMF, 5 equiv of $HCOONH_4$, 10% Pd/C, N_2, room temp, 30 min; (n) MeOH, argon, 4 equiv of 1-pyrazole-carboxamidine·HCl, 7 equiv of DIEA, room temp, 3 h; (o) separation of *S* and *R* diastereoisomers by preparative RP-HPLC, 30% CH_3CN in H_2O + 0.1% TFA.

To avoid the inconvenience with the β-carboxylic group protection, Asp was introduced into peptides as Fmoc-allylGly, following oxidative cleavage, and Arg was replaced during the synthetic steps by Orn(Cbz), following deprotection and guanidinylation. The final cyclopeptides were obtained as a mixture of two diastereoisomers (**I**, fast moving; **II**, slow moving according to their chromatographic t_R) because the fluorinated building block was introduced as a racemate, and they were separated by preparative RP-HPLC and obtained in all cases with a chromatographic purity greater than 98% after lyophilization. Final yields (calculated from the first building block) were not optimized and are given for each cyclopeptide in the Experimental Section.

The general synthetic approach for peptides **P1**−**P4** is shown for one example in Scheme 4, implying obvious differences in the sequential procedure. The ethyl ester hydrolysis of the intermediate dipeptide (condition c of Scheme 4) was accomplished by BBr_3 with almost quantitative yield because the presence of the *N*-phthaloyl protection is not compatible with basic conditions.

The synthesis of **P6** is illustrated in Scheme 5. For the acylation step of the dipeptide *N*-Me-α-TfmPhe-Orn(Cbz)-OtBu (condition b of Scheme 5), it was necessary to use 8 equiv of the corresponding bromide (50% yield). Owing to the instability of the bromide under long reaction conditions, we found it to be more convenient to add the reagent in successive portions. All other couplings and deprotections with proteinogenic amino acids proceeded with optimal yields until the completion of the pentapeptide. DCC/HOAT was a better coupling reagent than HATU (see Scheme 4); in fact, HATU often induces side products. For the azide reduction (condition e of Scheme 5), the Villarasa Sn complex[24] was very convenient because the Orn(Cbz) was totally unaffected.

In Vitro Biological Evaluation. The affinities of the six analogues **P1**−**P6** (in two diastereomeric forms **I** and **II**) to both $\alpha_v\beta_3$ and $\alpha_v\beta_5$ integrin receptors are listed in Table 1, in parallel with the reference cyclopeptides **R1**−**R4**. The IC_{50} values were measured as the concentrations of compounds required for 50% inhibition of Echistatin binding. The results of this test have brought to light unexpected differences within the group of reference compounds examined. In fact, on the basis of an inhibition test of vitronectin binding to α_v receptors, it was reported in the literature that amino acid substitution in the 5-position of an RGD cyclopentapeptide does not signifi-

Scheme 5. Synthesis of **P6-I** and **P6-II**, c[Arg-Gly-Asp-D-Phe-(*S* or *R*)-*N*-Me-α-TfmPhe][a]

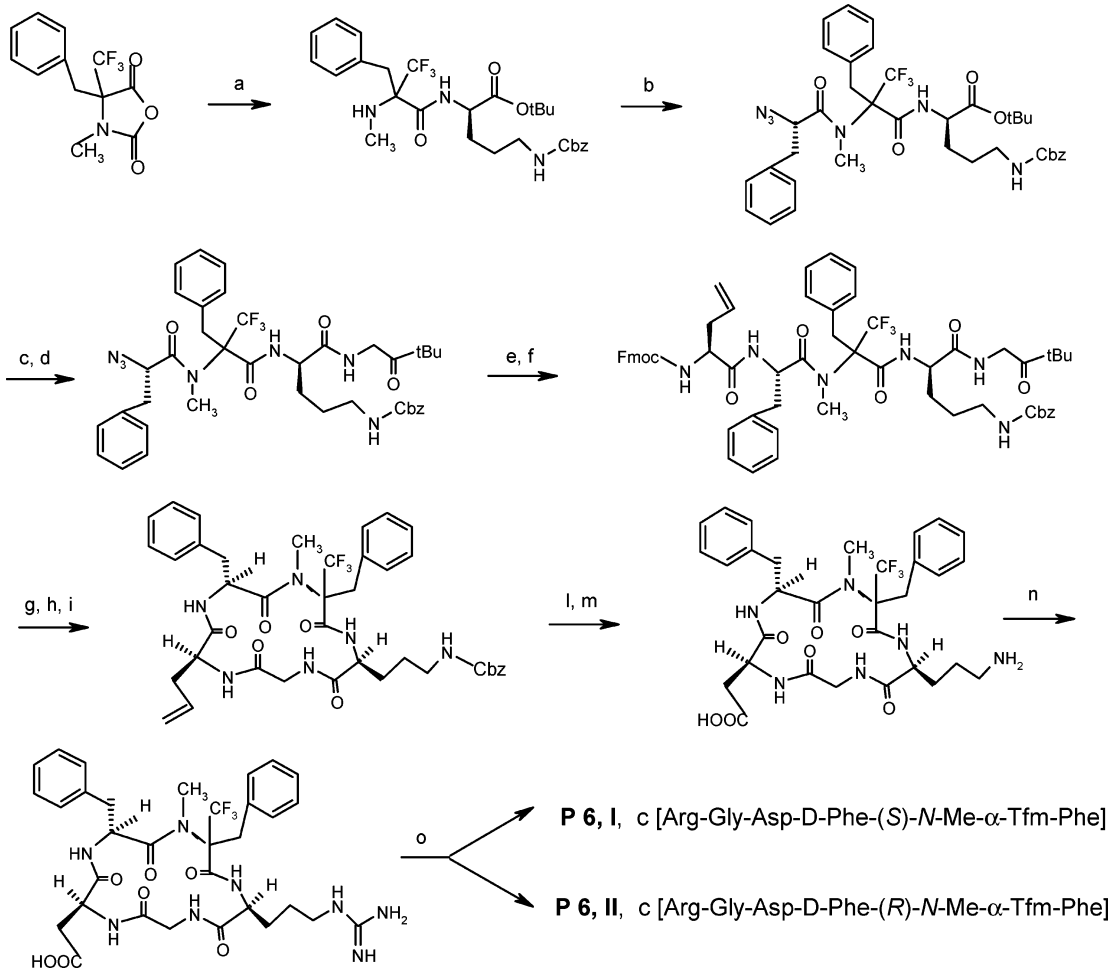

[a] Reagents and conditions: (a) HCl·Orn(Cbz)-OtBu, 2 equiv, TEA, 2 equiv, DCM, room temp, 1 night; (b) (i) 5 equiv of 2-azido-3-phenylpropionic acid, 7 equiv of bromoenamine, 2 equiv of collidine, DCM, argon, 10 min, (ii) 3 equiv of azidophenylpropionic acid, 5 equiv of bromoenamine, argon, 5 h; (c) 1:1 TFA/DCM, 1 h; (d) 1 equiv of HCl-H-Gly-OtBu, 1.2 equiv of HOAT, 1.2 equiv of DCC, 2 equiv of DIEA, 2 equiv of DCM, 2 h; (e) 1 equiv of [Et_3 NH] [$Sn(SPh)_3$], CH_3CN, room temp, 1 h; (f) 1 equiv of Fmoc-AllGly-OH, 1.2 equiv of HOAT, 1.2 equiv of DCC, DCM, 1.5 h; (g) 10 equiv of piperidine, DCM, room temp, 2 h; (h) 1:1 TFA/DCM, 1 h; (i) 10^{-3} M CH_3CN, 3 equiv of HOBT, 3 equiv of TBTU, 1% DIEA 20 min; (l) 10:0.7 acetone/3N H_2SO_4, 6 equiv of $KMnO_4$ aqueous solution, 0 °C → room temp, 1 night; (m) MeOH, 3 equiv of $HCOONH_4$, 10% Pd/C, N_2, room temp, 30 min; (n) MeOH, argon, 4 equiv of 1-pyrazole-carboxamidine·HCl, 4 equiv of DIEA, room temp, 3 h; (o) separation of *S* and *R* diastereoisomers by preparative RP-HPLC, 32% CH_3CN in H_2O + 0.1% TFA.

Table 1. Inhibition of Echistatin Binding to $\alpha_v\beta_3$ and $\alpha_v\beta_5$ Integrin Receptors[a]

		IC_{50}, nM (SD)	
		$\alpha_v\beta_3$	$\alpha_v\beta_5$
R 1	c(RGDfV)	195.9(16.8)	0.11(0.03)
R 2	c(RGDfMeV)	18.9(3.1)	0.13(0.009)
R 3	c(RGDfF)	10.31(1.24)	15.65(1.17)
R 4	c(RGDfMeF)	19.75(1.15)	19.81(1.39)
P1-I	c[RGDf-(*S*)αTfmV]	36.3(0.84)	3.4(0.07)
P1-II	c[RGDf-(*R*)αTfmV]	285.3(8.1)	42.8(0.5)
P2-I	c[RGDf-(*S*)αTfmF]	35.5(0.98)	
P2-II	c[RGDf-(*R*)αTfmF]	7237.9(1283.3)	93.5(9)
P3-I+II	c[RGDf-(*R*,*S*)αDfmF][b]	331.8(100.9)	5.5(0.8)
P4-I	c[RGD(*S*)αTfmfV]	237.1(64)	10.03(8.31)
P4-II	c[RGD(*R*)αTfmfV]	1017.8(347.8)	72.7(3.8)
P5-I	c[RG-(*S*)αTfmDfV]	>1000	>1000
P5-II	c[RG-(*R*)αTfmDfV]	>1000	>1000
P6-I	c[RGDf-(*S*)Me,αTfmF]	18.8(0.75)	7.7(0.16)
P6-II	c[RGDf-(*R*)Me,αTfmF]	704.4(9.2)	93.9(1.92)

[a] **R1**−**R4** are reference cyclopeptides and **P1**−**P6** are fluoromethylated cyclopeptides, each in its two diastereomeric forms **I** and **II**, related to the RP-HPLC retention times (**I** = fast moving; **II** = slow moving) [a] The two diastereoisomers were not separated.

cantly influence the activity.[25] This assumption is in contrast with our findings, and the discrepancy must be due to the different tests used. In our test, the peptide **R3** (containing Phe^5) was 20-fold more active than **R1** (containing Val^5) against $\alpha_v\beta_3$ but was 2 orders of magnitude less active against $\alpha_v\beta_5$. On the other hand, N-methylation of **R1** causes a 10-fold increase in the activity against $\alpha_v\beta_3$ (see **R2** vs **R1**) but it decreases the activity of **R3** (see **R4** vs **R3**).

The effects of α-trifluoromethylation follow the same trend: an increase of activity for cyclopeptides with Val in the 5-position but a decrease or equivalence for those with Phe in the same position (**P1-I** is 5-fold more active than **R1**, while **P2-I** and **P6-I** are either equipotent to or less active than **R3**). Unfortunately, for a full comparison, it was not possible to incorporate *N*-Me-α-TfmVal into the cyclopeptide because of the exceptional hindrance of this building block.

In all cases, inside each couple of the new analogues, isomer **I** (corresponding to the *S* configuration) was active whereas isomer **II** (corresponding to the *R* configuration) was much less active or totally inactive. In the case of peptide **P5** only, where the Tfm group is at the α-position of Asp^3, both isomers are devoided of activity. This is consistent with previous observations assigning to this moiety of the backbone utmost importance for the binding to α_v integrins. In fact, every substitution in the

Table 2. Interproton Distances (Å) from NOE Experiments and MD Simulations for the Backbone Protons of the Fluorinated (**P**) and Reference (**R**) Cyclopeptides[a]

	P1-I c[RGDf-(*S*)-αTfmV]		**P1-II** c[RGDf-(*R*)-αTfmV]		**R1** c(RGDfV)		**P6-I** c[RGDf-(*S*)-Me-αTfmF		**P6-II** c[RGDf-(*R*)-Me-αTfmF		**R4** c(RGDfMeF)	
i, *i* + 2	d_{exp} [b]	d_{calc} [c]	d_{exp}	d_{calc}	d_{exp}	d_{calc}	d_{exp}	d_{calc}	d_{exp}	d_{calc}	d_{exp} [d]	c_{calc}
1α···3N	zero NOE	5.4	zero NOE	5.1	zero NOE	5.1	zero NOE	4.8	nd[e]	5.2	*f*	5.5
1N···3N	4.0−4.5	4.5	4.0−4.5	3.9	4.0−4.5	4.3	3.5−4.0	3.7	3.5−4.0[g]	3.6	*f*	5.2
1N···4N	4.5−5.0	4.7	4.5−5.0	4.9	4.5−5.0	4.9	zero NOE	5.1	4.5−5.0	4.7	zero NOE	5.9
1α···4N	zero NOE	6.1	zero NOE	6.2	zero NOE	5.9	zero NOE	6.2	nd[e]	6.1	zero NOE	6.7
2N···4N	4.5−5.0	4.9	4.5−5.0	4.8	*h*	4.8	4.5−5.0	5.0	4.5−5.0	4.7	zero NOE	5.5
2α···4N	zero NOE	5.3, 5.2[i]	zero NOE	5.2, 5.5	zero NOE	5.1, 5.5	zero NOE	5.4, 5.0[g]	zero NOE	5.2, 5.4	zero NOE	5.6, 5.5

[a] The intra and the sequential α,N and N,N interactions are reported in the Supporting Information. They were found for all residues except for those involving Hα of Asp3 because the signal is overlapped by the water. [b] Measured by ROESY experiments in H_2O/D_2O (9:1) at pH 6.0 at 15 °C and converted into distances by using as reference the cross-peak of Gly CH2-α (1.75 Å). The values 4.5−5.0 Å indicate the limit of the detection. [c] MD simulations performed with explicit water and without constraints. The values were obtained from an average structure and from the last frame of the free MD, both energy-minimized (rms = 0.2 Å). [d] Measured in DMSO because in H_2O/D_2O (9:1) too many NH signals are overlapped and consequently no (*i*, *i* + 2) NOE peaks were detected. [e] Not detected because Hα is overlapped by the water signal. [f] Overlapped by the sequential interaction. [g] Partially overlapped by the sequential 1N···2N interaction. [h] Not detected because too close to the diagonal. [i] Pro-*R* and Pro-*S*, respectively.

proximity of the peptide bond Gly−Asp led to a drastic reduction of the activity, suggesting that close contact between this bond and the receptor is essential for the affinity.[26−28] Except for **P5**, the peptide **P4-I**, containing α-Tfm at the 4-position of the ring, is the least potent in the series.

Stereochemical Assignment. Two couples of diastereoisomers, couple **P1-I** and **P1-II** and couple **P6-I** and **P6-II**, endowed with interesting activities, were chosen for detection of the absolute configuration by NMR experiments.

The ^{1}H chemical shifts are quite similar in each pair of stereoisomers except for those of Val[5] and Phe[5]. For instance, NH and Hβ of Val[5] are more deshielded in **P1-I** than in **P1-II** (1.08 and 0.5 ppm, respectively), but this trend is not well reproduced in the two stereoisomers of **P6**. Consequently, the stereochemical assignment cannot be deduced from the chemical shift values, even though the shift variation can be attributed to the different orientations of the electronegative group CF_3. Only significant interproton distances, derived from nuclear Overhauser effect (NOE) experiments, can be used to determine the absolute configuration.

Because the stereocenter in question is the Cα of Val[5] and Phe[5] for the isomers of **P1** and **P6**, respectively, the most significant distances are those between these amino acids and the adjacent units Arg[1] and D-Phe[4]. Owing to the absence of the Hα proton in the amino acid at the 5-position, the comparison of the NOE data for the backbone protons did not give useful information (see Table 2), but the interactions involving protons of the side chains were more promising. Specifically, NOE cross-peaks involving NH and $CH_2\beta$ of Arg[1] with Hβ and the methyl groups of Val[5] were found in **P1-I** but not in its isomer **P1-II**. Similarly, NOEs connecting Hα and Hβ,γ of Arg[1] with Hβ and the aromatic protons of Phe[5] were found for **P6-I** but not for **P6-II** (Table 3). These interactions correspond to interproton distances, in agreement with the values derived from molecular dynamics (MD) simulations without NMR constraints of the *S* stereoisomers. The simulations of the *R* stereoisomers gave, for the same distances, values greater than 5 Å, in agreement with the detected zero NOE. The NOEs between D-Phe[4] and Val[5] or Phe[5] were not useful for the stereochemical assignment because the values are similar for both isomers.

Therefore, the *S* configuration can be assigned to **P1-I** and **P6-I** and the *R* configuration to **P1-II** and **P6-II**. Similar NOE interactions were also found for the known model compounds **R1** (c(RGDfV)) and **R4 (**c(RGDfMeF)), which show in the MD simulations the same orientation of the sidechains observed for the *S* stereoisomers **P1-I** and **P6-I** (Table 2).

Conformational Study. The 2D ROESY (rotating-frame Overhauser enhancement spectroscopy) experiments showed, for all the examined peptides, the expected sequential interactions and some significant medium-range (*i*, *i* + 2) cross-peaks between protons of Arg[1] and protons of Asp[3] and D-Phe[4]. Weaker interactions were also found between NH protons of Gly[2] and D-Phe[4]. The values are similar for both stereoisomers of **P1** and **P6** and for the model peptide **R1**. The interproton distances derived from the medium-range interactions are reported in Table 2, whereas those for the sequential and the intraresidue interactions are reported in the Supporting Information (Tables S1 and S2). The other known cyclopeptide **R4**, considered as a model for **P6** isomers, unfortunately did not give satisfactory results because the overlapping of too many signals in the ROESY spectrum in water did not allow detection of any (*i*, *i* + 2) NOE cross-peak, and in DMSO no (*i*, *i* + 2) NOE interaction was found. The spectra in DMSO of the other peptides are substantially similar to those in water.

Free MD simulations with both explicit water or distant-dependent $\epsilon = 4.0r$ confirmed these findings. The distance values d_{calc} reported in Table 2 are in very good agreement with the experimental ones. They were obtained by free MD simulations with explicit water (see Experimental Section). Because conformational motions are also expected to occur for cyclic peptides, the simulations without NMR constraints represent the best approach to compare experimental with calculated data. MD simulations with NOE constraints were also performed, and the values were very similar to those reported in Table 2.

An ensemble of 20 structures obtained by the free-MD with explicit water is reported in Figure 2 for one peptide as an example, showing that backbones are perfectly superimposed. Similar results were obtained for the other molecules and also with longer simulations and with $\epsilon = 4r$.

To better investigate the mobility of these peptides, a 150 ps MD simulation with $\epsilon = 4r$ was carried out at 300 K and without application of any NMR constraint. During the simulation time of the dynamics, the values of Φ and Ψ angles were sampled every picosecond and the Ramachandran plots for all six peptides were examined. The Φ and Ψ angles of both **P1** stereoisomers and of the model peptide **R1** showed small variations during the free MD. **P1-I**, **P6-I**, and **P6-II** are reported in Figure 3 as examples. In Figure 3a the spread of conformations of **P1-I** is very small. The values of Φ and Ψ are around +90° and −90° and are similar for the three peptides, except for Φ_5, Ψ_4, and Ψ_5. The fourth and fifth units appear diversified as a consequence of the different structure at Val[5] Cα. In the

Table 3. Interproton Distances (Å) from NOE Experiments and MD Simulations for the Side Chain Protons of the Fluorinated (**P**) and Reference (**R**) Cyclopeptides[a]

	P1-I c[RGDf-(*S*)-αTfmV]		**P1-II** c[RGDf-(*R*)-αTfmV]		**R1** c(RGDfV)	
	d_{exp} [b]	d_{calc} [c]	d_{exp}	d_{calc}	d_{exp}	d_{calc}
1α···5*β*	zero NOE	5.0	zero NOE	5.0	nd[d]	4.9
1N···5*β*	2.5−3.5	2.4	zero NOE	4.8	2.5−3.5	2.4
1N···5Me[e]	3.5−4.5	3.7, 4.2	zero NOE	5.0, 5.2	3.5−4.5	3.7, 4.2
1*β*/*γ*···.5N	zero NOE	>6[f]	zero NOE	>6[f]	zero NOE	>6[f]
1*β*[g]···5Me	4.5−5.0[e]	3.6	zero NOE	5.4	4.5−5.0	4.0
1*β*′···.5Me	4.5−5.0[e]	4.4	zero NOE	6.4	4.5−5.0	5.1
4α···5N	nd[d]	2.1	nd[d]	2.2	nd[d]	2.2
4*β*···5N	3.5−4.5	4.2	3.5−4.5	4.5	4.5−5.0	4.5
4*β*′···5N	3.5−4.5	4.1	3.5−4.5	4.5	4.5−5.0	4.6
	P6-I c[RGDf-(*S*)-Me-αTfmF]		**P6-II** c[RGDf-(*R*)-Me-αTfmF]		**R 4** c(RGDfMeF)	
	d_{exp} [b]	d_{calc} [c]	d_{exp}	d_{calc}	d_{exp}	d_{calc}
1α···5*ββ*′	zero NOE	6.1, 4.9[e]	nd[d]	5.0, 5.1	zero NOE	6.0, 5.1
1N···5*β*	3.5−4.0	3.7	4.5−5.0	4.7	3.5−4.0	3.9
1N···5*β*′	2.5−3.5	2.4	4.5−5.0	4.6	2.5−3.5	2.4
1*βγ*···.5NMe	zero NOE	>6[f]	zero NOE	>6[f]	zero NOE	>5.5[f]
1α···5arom[h]	4.0−4.5	4.5	nd[d]	>7.0	4.5−5.0	4.0
1*ββ*′···5arom[h]	2.5−3.5	2.5, 4.1[e]	zero NOE	>7.0	3.5−4.5	2.7, 4.0[e]
1*γγ*′···5arom[h]	3.5−4.5	2.7, 4.2[e]	zero NOE	>7.0	zero NOE	>5.5[f]
4α···5NMe	2.5−3.5	2.6	2.5−3.5	2.5	2.5−3.5	2.6
4*ββ*′···5NMe	nd[d]	4.7, 4.8[e]	4.5−5.0[h]	4.9, 5.0	2.5−3.5[h]	2.6, 3.6

[a] The intra and the sequential α,N and N,N interactions are reported in the Supporting Information. They were found for all residues except for those involving Hα of Asp3 because the signal is overlapped by the water. [b] Measured by ROESY experiments in H_2O/D_2O (9:1) at pH 6.0 at 15 °C and converted into distances by using as reference the cross-peak of Gly CH2-α (1.75 Å). The values 4.5−5.0 Å indicate the limit of the detection. [c] MD simulations performed with explicit water and without constraints. The values were obtained from an average structure and from the last frame of the free MD, both energy-minimized (rms = 0.2 Å). [d] Not detected because Hα is close to or overlapped by the water signal. [e] The protons have the same chemical shift. The values of d_{calc} stand for pro-*R* and pro-*S*, respectively. [f] All the distances for *β* and *γ* protons are greater than 6 Å (for **R4**, they are greater than 5.5 Å). [g] *β* and *β*′, *γ* and *γ*′ stand for low field and upfield, respectively. [h] The aromatic protons were not assigned. The values of d_{calc} stand for protons at the ortho positions. [i] *β* and *β*′ protons are very close.

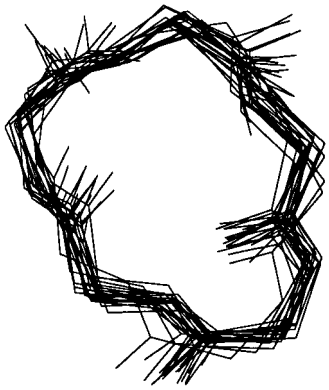

Figure 2. The 20 superimposed backbone conformations of **P6-I** obtained by free MD with explicit water (rms = 0.2 Å).

case of the **P6** isomers and for the model peptide **R4**, the spread of conformations is slightly larger, as shown in Figure 3b,c; the Ψ angles have different values in the two stereoisomers of **P6**, while the Φ ones are more constant. The plots of the model peptides **R1** and **R4** appear quite similar to those of the *R* stereoisomers **P1-II** and **P6-II**, respectively.

RGD cyclic pentapeptides containing a D-amino acid usually exhibit a *β*II′/*γ* conformation with the D-Aaa in the $i + 1$ position of the *β*-turn and with the Gly in the $i + 1$ position of the *γ* turn.[10] We measured the distances between NH of Arg[1] and CO of Asp[3] in order to see the possible existence of a hydrogen bond, which defines the *β*II′-turn. For the couple **P1-I** and **P1-II** and for the model **R1**, only 25 of the 150 structures obtained by the free simulations are consistent with the presence of such a hydrogen bond (≤2.8 Å). The same procedure, applied to the distance between NH of Asp[3] and CO of Arg[1], showed that all the structures present distances compatible with the hydrogen bond typical of a *γ*-turn. Therefore, the *γ*-turn Arg[1]-Gly[2]-Asp[3] appears more stable than the *β*II′-turn Arg[1]-Val[5]-D-Phe[4]-Asp[3], and the presence of CF_3 at Cα of Val[5] does not significantly affect the ring shape. The Φ and Ψ angles, monitored during the free MD simulations, did not display values consistent with the presence of *β*II′-turns,[29] thus confirming the above results. On the other hand, the *β*II′-turn is almost absent in the pair of isomers **P6-I** and **P6-II** as well as in the model peptide **R4**, while 25 of the 150 structures showed distance values consistent with the presence of a hydrogen bond typical of the *γ*-turn. The presence of the methyl group at the nitrogen atom of Phe[5] seems to induce a slight lengthening of the distance between the NH of Arg[1] and the oxygen of Asp[3], but this small variation was not detected by the NOEs of the backbone protons. Similar results were also found by Kessler in the case of **R2**.[12] The distance between the C*β* atoms of Arg[1] and Asp[3], obtained from the average over the free MD trajectory, is 7.7−7.8 Å in the case of the two isomers **P1** and **R1** and is 8.0−8.2 Å for the pairs **P6** and for the model **R4**. This might be in line with the more flexible *γ*-turn, even if the small difference did not allow us to draw definite conclusions.

The conformations of the side chains are different in the two stereoisomers of both **P1** and **P6**, as can be deduced from the NOE values reported in Table 3 and confirmed by the calculations (see the discussion under Stereochemical Assignment). The Arg[1] side chain is preferentially oriented toward the Val[5] (or Phe[5]) residue in the *S* stereoisomers as well as in the model peptides **R1** and **R4.** By contrast, the two side chains of the *R* stereoisomers point in opposite directions. Consequently, the important space between the side chains of Arg[1] and Asp[3] becomes larger in **P1-I** and **P6-I** with respect to the corresponding *R* stereoisomers **P1-II** and **P6-II** (see Figure 4). The different

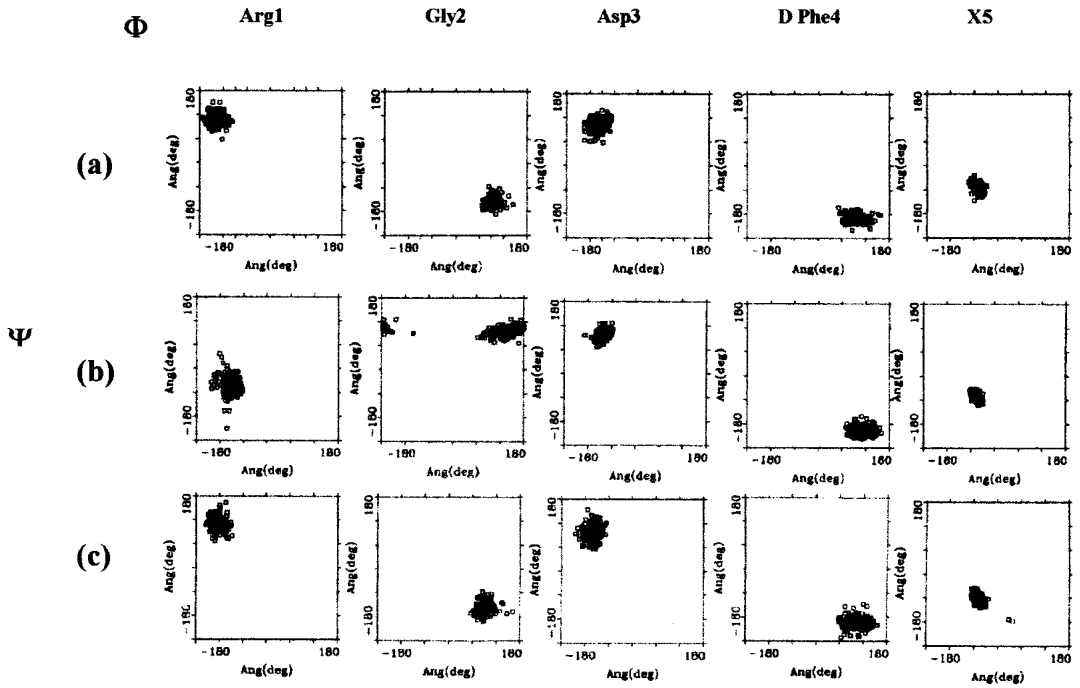

Figure 3. Ramachandran plot is shown for each of the five amino acids of (a) **P1-I**, (b) **P6-I**, (c) **P6-II**.

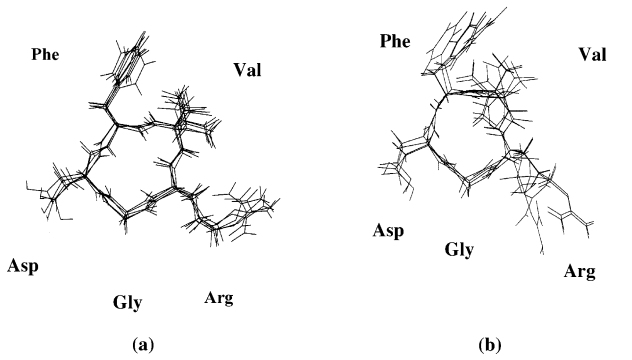

Figure 4. The 5 of the 150 structures obtained by free MD with $\epsilon = 4r$ for (a) **P1-I** and (b) **P1-II**. The 150 structures were all examined, but only 5 were reported for clarity of the drawing.

conformations of the pharmacophoric side chains in the two stereoisomers might thus explain the difference in their activities.

Conclusion

It is possible to draw interesting observations from the comparison between Kessler's cyclic peptides and their corresponding analogues containing one α-Tfm-Aaa at three different positions of the ring. The effect of the introduction of the Tfm group is quite different for different model peptides: **P1-I**, containing α-TfmVal[5], is 5-fold more active than its model peptide **R1**, whereas **P2-I** and **P6-I**, containing α-TfmPhe[5] and *N*-Me-α-TfmPhe[5], respectively, were less active than or equivalent to their model peptides **R3** and **R4**.

The results of conformational analysis revealed only minimal difference among the backbone conformations of **P** and **R** peptides, yet showing for **P6** very subtle deviations of the pharmacophoric side chains. The increased activity of the N-methylated **R2** vs **R1** has been explained in the literature[12] by a change of conformation from a βII′/γ turn to a more flexible $\gamma_t/\gamma/\gamma_t$ arrangement because the hydrogen bond between Arg[1]-NH and Asp[3]-CO is disturbed by the *N*-methyl group of the valine residue. The mechanism of this hindrance was later attributed to a subtle rotation of the ω angle of D-Phe-Val from an exact trans conformation.[30]

These variations, however, do not give a satisfactory explanation for the profound difference in the behavior between the analogues containing Val[5] and those containing Phe[5]: α-trifluoromethylation and N-methylation increase the activity in the former but produce only marginal effects in the latter. The different behavior of the Phe[5] series must be attributed to another stronger effect that is prevalent, outweighing the others. With the exchange of the amino acid in the 5-position being the only obvious feature that discriminates between **R1** and **R3**, it is reasonable to infer that once in the bound state at the receptor site the benzyl residue could induce different interactions compared to the isopropyl. Another evidence reinforcing this interpretation is the dramatic loss of activity of **P2-II**, where the phenylalanine is in the *R* configuration (7237 vs 35), whereas in **P1-II**, with valine in the *R* configuration, the loss of activity is much less pronounced (285 vs 36). The great difference between **R1** and **R3** had not been shown by the test of inhibition of vitronectin previously used but only by the test with echistatin; the difference in the mode of binding to the receptors between the two proteins used in the test can account for different results.

On the basis of this study, we may assume that introduction of a α-TfmAaa into suitable positions of conformationally well-defined and rather rigid cyclopeptides, like Kessler's RGD, does not imply loss of activity and that the residue D-Phe-α-TfmAaa behaves in a manner similar to that of the parent residue D-Phe-*N*-Me-Aaa. Then, cyclopeptides containing the α-Tfm group at the 5-position could be considered potent hydrophobic RGD mimetics.

Different implications could be found with different model peptides, and in any case, modification of the pharmacokinetic behavior, such as improved absorption and duration of action, is the most likely advantage expected. Furthermore, the ^{19}F atom serves as a highly specific label for spectroscopic investigation of protein−protein interaction and metabolism. The feasibility of the site-specific incorporation of α-trifluoroalkylamino acids into peptides or hydrophobic folds of large proteins may provide

valuable tools for modifying their physical properties in the process of new drug discovery. Very recently, an exhaustive review appeared about the application of fluorinated amino acids to the rational design of structural motifs and protein interfaces.[31]

Experimental Section

Materials and Methods. Trifluoropyruvate was purchased from Apollo Scientific, Stockport, U.K. DCM was distilled over P_2O_5 and stored under argon. 1-Bromo-*N*,*N*-2-trimethyl-1,1-propenylamine was synthesized by a method described in the literature[32] and stored in vials as a 1 M solution in DCM at −18 °C, under argon, for several months. 2-Azido-3-phenylpropionic acid was synthesized by diazotranfer reaction from D-Phe, as described by Alper et al.[33] TLC was routinely carried out to monitor reactions using suitable mixtures of $CHCl_3$/MeOH or hexane/EtOAc, and the products were located with UV light (250 nm), ninhydrin, $KMnO_4$, or Pancaldi reagent, according to their chemical structures. Alternatively, the reaction kinetics was followed by RP-HPLC. Analytical and preparative liquid chromatography were carried out on a Waters 600 HPLC system, UV detector at 220 nm, using mixtures of CH_3CN/water + 0.1% TFA as mobile phases and the following columns: Ultrasphere ODS (5 μm, 10 μm × 250 μm), Beckman and Alltima C_{18} (10 μm, 22 μm × 250 μm), Alltech. Routine ^{1}H and ^{19}F NMR spectra were recorded on Bruker spectrometers AC 300 or ARX 400. Chemical shifts (δ) are reported in ppm of the applied field. $SiMe_4$ was used as an internal standard for ^{1}H spectra in DMSO-d_6 and CD_3OD, and the residual water signal, set at δ = 4.80 ppm, was used for aqueous solutions. CF_3COOH was used as the internal standard for ^{19}F nucleus.

c[RGDf-(*S* or *R*)-α-TfmV] (P1-I and P1-II). Total yield 4.2%. **I** isomer: HPLC, 30% CH_3CN, t_R = 19.93 min. ^{1}H NMR (D_2O) δ: 7.37−7.25 (m, 5 H arom); 4.88 (q, CHα-Asp); 4.76 (q, CHα-Phe); 4.50 (q, CHα-Arg); 4.13 and 3.47 (2 dd, CH_2-Gly, J = 8.41, 8.13 Hz); 3.20 (q, *N*-CH_2-Arg); 3.08−2.69 (m, CH_2-Phe + CH_2-Asp); 2.33 (m, CHβ-Val); 1.87−1.60 (m, 2 CH_2-Arg); 1.08 (m, 2 CH_3-Val). ^{19}F NMR (D_2O) δ: 9.53 (α-CF_3). MS (MALDI) calcd for $C_{27}H_{37}F_3N_8O_7$, 642.64; found (M + H^+), 643.06. **II** isomer: HPLC, 30% CH_3CN, t_R = 21.45 min. ^{1}H NMR (D_2O) δ: 7.37−7.30 (m, 5 H arom); 4.87 (q, CHα-Asp); 4.72 (q, CHα-Phe); 4.56 (q, CHa-Arg); 4.13−3.54 (m, CH_2-Gly); 3.17 (m, *N*-CH_2-Arg + 1 Hβ, Phe); 2.98−2.59 (m, 1 Hβ, Phe + Hβ-Val + CH_2-Asp); 1.88−1.60 (m, 2 CH_2-Arg); 1.18 and 0.85 (m, 2 CH_3-Val). ^{19}F (D_2O) δ: 8.32 (α-CF_3). MS (MALDI) found (M + H^+), 643.16.

c[RGDf-(*S* or *R*)-α-TfmF] (P2-I and P2-II). Total yield 5.6%. **I** isomer: HPLC, 34% CH_3CN, t_R = 21.32 min. ^{1}H NMR (D_2O) δ: 7.27−7.17 (m, 10 H arom); 4.82 (t, CHα-Asp); 5.00 (t, CHα-Phe); 4.19 (t, CHα-Arg); 3.90 and 3.40 (2d, CH_2-Gly); 3.60−2.55 (m, 2 CH_2-Phe + CH_2-Asp); 3.05 (m, *N*-CH_2-Arg); 1.62−1.23 (2 CH_2-Arg). ^{19}F NMR (CD_3OD) δ: 5.18 (α-CF_3). MS (MALDI) calcd for $C_{31}H_{37}F_3N_8O_7$, 690.76; found (M + H^+), 691,14. **II** isomer: HPLC, 34% CH_3CN, t_R = 25.93 min. ^{1}H NMR (D_2O) δ: 7.30−7.15 (m, 10 H arom); 4.85 (dd, CHα-Asp); 4.65 (t, CHα-Phe); 4.05 and 3.47 (2 d, CH_2-Gly); 3.85 and 3.22 (2 d, CH_2-Phe); 3.15 (m, *N*-CH_2-Arg); 2.60−2.50 (m, CH_2-Phe + CH_2-Asp); 1.81−1.55 (m, 2 CH_2-Arg). ^{19}F NMR (CD_3OD) δ: 4.17 (s, α-CF_3). MS (MALDI) found (M + H^+), 691.13.

c[RGDf-(*S*,*R*)-α-Dfm-F] (P3-I and P3-II). Total yield 10.2%. HPLC, 30% CH_3CN, t_R = 21.32 min for **I** and 22.69 min for **II** (the two diastereoisomers were not separated because they were too close each other in the chromatographic system used). ^{1}H NMR (CD_3OD) δ: 8.02−7.05 (m, NH); 7.35−7.15 (m, 10 H arom); 6.42−5.06 (2 t, H-CF_2, J = 53.49, 54.85); 4.75−4.32 (m, 3 CHα); 4.30−4.02 (dd, CH_2-Gly, one isomer); 3.68−3.34 (dd, CH_2-Gly, other isomer); 3.30−2.52 (m, 2 CH_2-Phe + CH_2-Asp + *N*-CH_2-Arg); 2.07−1.45 (m, 2 CH_2-Arg). ^{19}F (DMSO-d_6) δ: from −52.8 to −57.0 (α-CHF_2). MS (MALDI) calcd for $C_{31}H_{38}F_2N_8O_7$, 672.77; found (M + H^+), 673.14.

c[RGD-(*S* or *R*)-α-TfmFV) (P4-I and P4-II). Total yield 6.7%. **I** isomer: HPLC, 30% CH_3CN, t_R =17.19 min. ^{1}H NMR (D_2O) δ 7.40−7.34 (m, 5 H arom); 4.89 (m, CHα-Asp); 4.30−4.19 (m, CHβ-Phe + CHα-Val + CHα-Arg); 3.75−3.58 (m, CHβ-Phe + CH_2-Gly); 3.30−2.84 (m, *N*-CH_2-Arg + CH_2Asp); 2.35−1.51 (m, CHβ-Val + 2 CH_2-Arg); 0.88−0.73 (m, 2 CH_3-Val). MS (MALDI) calcd for $C_{27}H_{37}F_3N_8O_7$, 642.64; found (M + H^+), 643.28. **II** isomer: HPLC, 30% CH_3CN, t_R = 22.17 min. ^{1}H NMR (D_2O) δ: 7.37−7.21 (m, 5 H arom); 4.76 (m, CHα−Asp); 4.24 (m, CHα-Val); 4.08 (m, CHα-Arg); 3.74−3.34 (m, CH_2-Gly + CH_2-Phe); 3.25−3.22 (m, *N*-CH_2Arg); 3.03−2.78 (m, CH_2-Asp); 2.10−1.60 (m, CHβ-Val + 2 CH_2-Arg); 0.94−0.84 (m, 2 CH_3-Val). MS (MALDI) found (M + H^+), 643.12.

c[RG-(*S* or *R*)-α-TfmDfV] (P5-I and P5-II). Total yield 4.2%. **I** isomer: HPLC, 22% CH_3CN, t_R = 20.76 min. ^{1}H NMR (DMSO-d_6 + D_2O) δ: 7.22−7.15 (m, 5 H arom); 4.69 (t, CHα-Phe); 4.09 (d, CHα-Val); 3.87 (t, CHα-Arg); 4.24 and 3.52 (2 d, CH_2-Gly, J = 15.61 Hz); 3.23−2.83 (m, CH_2-Phe + CH_2-Asp + *N*-CH_2-Arg); 1.96 (m, CHβ-Val); 1.75−1.31 (m, 2 CH_2-Arg); 0.69−0.64 (2 d, 2 CH_3-Val). MS (MALDI) calcd for $C_{27}H_{37}F_3N_8O_7$, 642.64; found (M + H^+), 643.2. **II** isomer: HPLC, 22% CH_3CN, t_R = 25.44 min. ^{1}H NMR (DMSO-d_6 + D_2O) δ: 7.19−7.00 (m, 5 H arom); 4.50 (t, CHα-Phe); 4.05 (t, CHα-Val); 4.00−3.59 (m, CH_2-Gly); 3.55 and 3.24 (2 d, CH_2-Asp, J = 15.5 Hz); 3,05−2.84 (m, CH_2-Phe + *N*-CH_2-Arg); 1.88−1.41 (m, CHβ-Val + 2 CH_2Arg); 0.84 (m, 2 CH_3-Val). MS (MALDI) found (M + H^+) 643.2.

c[RGDf-(*S* or *R*)-*N*-Me-α-TfmF] (P6-I and P6-II). Total yield 4.5%. **I** isomer: HPLC, 40% CH_3CN, t_R = 11.97 min. ^{1}H NMR (D_2O) δ 7.40−7.26 (m, 10 H arom); 5.16 (t, CHα-Asp); 4.78 (t, CHα-Phe); 4.30 (t, CHα-Arg); 4.05 and 3.47 (2 d, CH_2-Gly, J = 14.27 Hz); 3.65−3.34 (2 d, CH_2-Phe, J = 14.27 Hz); 3.19 (s, *N*-CH_3); 3.17−2.62(m, *N*-CH_2-Arg + CH_2-Asp + CH_2-Phe); 1.7−1.23(2 CH_2-Arg). MS (MALDI) calcd for $C_{32}H_{39}F_3N_8O_7$, 704.79; found (M + H^+), 705.36. **II** isomer: HPLC, 40% CH_3CN, t_R = 13.89 min. ^{1}H NMR (D_2O) δ: 7.36−7.21 (m, 10 H arom); 5.00 (dd, CHα-Asp); 4.71 (t, CHα-Phe); 4.07 and 3.57 (2 d, CH_2-Gly); 3.92 and 3.37 (2 d, CH_2-Phe); 3.22 (m, *N*-CH_2-Arg); 2.94 (s, *N*-CH_3); 2.71−2.51 (m, CH_2-Phe + CH_2-Asp); 1.89−1.50 (m, 2 CH_2-Arg). MS (MALDI) found (M + H^+), 705.34.

NOE Experiments. The NMR spectra were recorded on a Bruker AMX 600 spectrometer operating at a frequency of 600.13 MHz for the ^{1}H nucleus. The chemical shifts (δ) were measured in ppm and referenced to the residual water signal set at 4.87 ppm for 15 °C and to DMSO-d_6 set at 2.50 ppm. The experiments were performed in DMSO at 25 °C and in H_2O/D_2O (90:10) at 25, 15, and 5 °C, pH 4.5−6.0. The concentrations were 2−3 mM. The sequential assignments in the peptide backbones were performed following the known strategy for protein structure.[34] The procedure was established by using a series of TOCSY (total correlation spectroscopy) and NOESY and ROESY experiments in H_2O/D_2O (9:1). NOESY and ROESY spectra were acquired in the phase-sensitive TPPI mode, with 1K × 1K complex free induction decays (FIDs), spectral width of 9090.909 Hz for water solvent, recycling delay of 1.3 s, 48−64 scans, and mixing times from 150 to 300 ms. TOCSY and ROESY spectra were recorded with the use of an MLEV-17 spin-lock[32] pulse (field strength 11 360 and 6250 Hz, respectively; 60 ms total duration). All spectra were transformed and weighted with a 90° shifted sine-bell-squared function to 1K × 1K real data points. For the ROESY spectra in water, the solvent suppression was achieved by a presaturation technique, placing the carrier frequency on the H_2O resonance, whereas the NOESY spectra were measured by using p11-homo pulse programs, capable of suppressing the water signal and minimizing the magnetization loss due to saturation transfer.

Molecular Modeling. Molecular models were built using a Silicon Graphics 4D35GT workstation running the Insight II & Discover software. Molecular mechanics (MM) and molecular dynamics (MD) were carried out using the cvff force field. The starting geometry of the peptides was generated using standard bond lengths and angles. The MD calculations were performed with relative permittivity $\epsilon = 4.0r$ and with explicit water. At the first step of the simulation with $\epsilon = 4.0r$, a minimization by Discover with a steepest-descendent algorithm was carried out, followed by conjugate gradient minimization. Then 150 ps of restrained MD

simulation was performed at a constant temperature of 300 K, sampling the trajectory every picosecond. The last frame was taken as the starting structure for a 150 ps free MD simulation at 300 K, sampling the Φ and Ψ angles every picosecond. The last frame of the free MD was subjected to a further minimization and compared with an energy-minimized average structure and with those derived from the restrained MD simulation, obtaining substantially the same results (rms = 0.2 Å). The simulations with explicit water were performed by surrounding the system by a sphere of water molecules with radius of 25 Å. Then 20 ps of restrained molecular dynamics simulations were carried out at 300 K and the last frame was taken as a starting structure for 20 ps of free MD simulations. The last frame of the free MD was subjected to a further minimization and compared with the energy-minimized average structure of the 20 derived from the free MD (rms = 0.2 Å), obtaining the distances reported in Table 1.

Solid-Phase Receptor-Binding Assay. The receptor binding assays were performed as described by Kumar et al.[35] Purified $\alpha_V\beta_3$ and $\alpha_V\beta_5$ receptors (Chemicon International Inc., Temecula, CA) were diluted to 500 and 1000 ng/mL, respectively, in coating buffer [20 mM Tris-HCl (pH 7.4), 150 mM NaCl, 2 mM $CaCl_2$, 1 mM $MgCl_2$, and 1 mM $MnCl_2$]. An aliquot of diluted receptors (100 μL/well) was added to 96-well microtiter plates and incubated overnight at 4 °C. Coating solution was removed, and an amount of 200 μL of blocking solution (coating buffer plus 1% BSA) was added to the wells and incubated for an additional 2 h at room temperature. After incubation, the plates were rinsed three times with 200 μL of blocking binding solution and incubated for 3 h at room temperature with 0.05 nM and 0.1 nM [^{125}I]echistatin (Amersham Pharmacia) for $\alpha_V\beta_3$ and $\alpha_V\beta_5$ receptor binding assays, respectively. After incubation, the plates were sealed and counted in the γ-counter (Packard). The IC_{50} values were calculated as the concentrations of compounds required for 50% inhibition of echistatin binding. Each data point is a result of the average of triplicate wells and was analyzed by nonlinear regression analysis with the Prism GraphPad program.

Acknowledgment. This work was partially supported by Sigma-Tau, Rome, Italy, and by the University of Milano and MIUR (Funds COFIN-2003 and FIRB-2001).

Supporting Information Available: Table S1 listing ^{1}H chemical shifts and Table S2 listing interproton distances. This material is available free of charge via the Internet at http://pubs.acs.org.

References

(1) Welch, J. T. Advances in the preparation of biologically active organofluorine compounds. *Tetrahedron* **1987**, *43*, 3123−3197.
(2) Sewald, N.; Burger, K. Synthesis of β-Fluorine-Containing Amino Acids. In *Fluorine-Containing Amino Acids*; Kukhar, V. P., Soloshonok, V. A., Eds.; Wiley: New York, 1995; p 139.
(3) Koksch, B.; Sewald, N.; Jakubke, H. D.; Burger, K. Synthesis and Incorporation of α-Trifluoromethyl-Substituted Amino Acids into Peptides. In *Biochemical Frontiers of Fluorine Chemistry*; Ojima, I., McCarthy, J. R., Welch, J. T., Eds.; ACS Symposium Series 639; American Chemical Society: Washington, DC, 1999; p 42.
(4) Hollweck, W.; Sewald, N.; Michel, T.; Burger, K. C-Terminal incorporation of α-trifluoromethyl-substituted amino acids into peptides via in situ deprotection of *N*-Teoc derivatives. *Liebigs Ann./Recl.* **1997**, 2549−2551.
(5) Burger, K.; Mütze, K.; Hollweck, W.; Koksch, B.; Kuhl, P.; Jakubke, H. D.; Riede, J.; Schier, A. Untersuchungen zur proteasekatalysierten und chemischen Peptidbindungs-knüpfung mit α-trifluoromethyl-substituierten α-Aminosäuren (Investigations of protease catalysis and chemical peptide binding with α-trifluoromethyl-substituted α-amino acids). *J. Prakt. Chem/Chem.-Ztg.* **1993**, *335*, 321−331.
(6) Sewald, N.; Hollweck, W.; Mütze, K.; Schierlinger, C.; Seymour, L. C.; Gaa, K.; Burger, K.; Koksch, B.; Jakubke, H. D. Peptide modification by introduction of α-trifluoromethyl substituted amino acids. *Amino Acids* **1995**, *8*, 187−194.
(7) Koksch, B.; Sewald, N.; Hoffmann, H. J.; Burger, K.; Jakubke, H. D. Proteolitically stable peptides by incorporation of α-Tfm-amino acids. *J. Pept. Sci.* **1997**, *3*, 157−167.
(8) Dal Pozzo, A.; Muzi, L.; Moroni, M.; Rondanin, R.; de Castiglione, R.; Bravo, P.; Zanda, M. Synthesis of RGD analogues containing α-Tfm-arginine as potential fibrinogen receptor antagonists. *Tetrahedron* **1998**, *54*, 6019−6028.
(9) Dal Pozzo, A.; Dikovskaya, K.; Moroni, M.; Fagnoni, M.; Vanini, L.; Bergonzi, R.; de Castiglione, R.; Bravo, P.; Zanda, M. Synthesis of RGD analogues containing α-trifluoromethylaspartic acid as potential fibrinogen receptor antagonists. *J. Chem. Res., Synop.* **1999**, 468−469, 1980−1991.
(10) Haubner, R.; Gratias, R.; Diefenbach, B.; Goodman, S. L.; Jonkzyc, A.; Kessler, H. Cyclic RGD peptides containing β-turn mimetics. *J. Am. Chem. Soc.* **1996**, *118*, 7461−7472.
(11) Haubner, R.; Finsinger, D.; Kessler, H. Stereoisomeric peptide libraries and peptidomimetics for designing selective inhibitors of the $\alpha_v\beta_3$ integrin for a new cancer therapy. *Angew. Chem., Int. Ed.* **1997**, *36*, 1374−1389.
(12) Dechantreiter, M. A.; Planker, E.; Mathä, B.; Lohof, E.; Hölzemann, G.; Jonkzyk, A.; Goodman, S. L.; Kessler, H. *N*-Methylated cyclic RGD peptides as highly active and selective $\alpha_v\beta_3$ integrin antagonists. *J. Med. Chem.* **1999**, *42*, 3033−3040.
(13) Goodman, S. L.; Hölzemann, G.; Sulyok, G. A. G.; Kessler, H. Nanomolar small molecule inhibitors for $\alpha_v\beta_6$, $\alpha_v\beta_5$, and $\alpha_v\beta_3$ integrins. *J. Med. Chem.* **2002**, *45*, 1045−1051.
(14) Marinelli, L.; Lavecchia, A.; Gottschalk, K. E.; Novellino, E.; Kessler, H. Docking studies on $\alpha_v\beta_3$ integrin ligands: pharmacophore refinement and implications for drug design. *J. Med. Chem.* **2003**, *46*, 4393−4404.
(15) Marinelli, L.; Gottschalk, K. E.; Meyer, A.; Novellino, E.; Kessler, H. Human integrin $\alpha_v\beta_5$: homology modeling and ligand binding. *J. Med. Chem.* **2004**, *47*, 4166−4177.
(16) Smith, J. W. Cilengitide Merck. *Curr. Opin. Invest. Drugs* **2003**, *4*, 741−745.
(17) Bey, P.; Vevert, J.; Van Dorsselaer, V.; Kolb, M. Direct synthesis of halogenomethyl-α-amino acids from the parent α-amino acids. *J. Org. Chem.* **1978**, *44*, 2732−2742.
(18) Burger, K.; Gaa, K. Eine effiziente Synthese für α-Trifluoromethyl-substituierte ω-Carboxy-α-aminosäuren (An effective synthesis of α-trifluoromethyl-substituted ω-carboxy-α-amino acids). *Chem. Ztg.* **1990**, *114*, 101−103.
(19) Burger, K.; Hollweck, W. Synthesis of *N*-Allyl-α-trifluoromethyl-α-amino acids and incorporation into peptides. *Synlett* **1994**, 751−753.
(20) Dal Pozzo, A.; Bergonzi, R.; Ni, M. H. N-Protected amino acids bromides: efficient reagents for the incorporation into peptides of extremely hindered α,α-dialkyl- and α-fluoroalkyl-amino acids. *Tetrahedron Lett.* **2001**, *42*, 3925−3927.
(21) Meldal, M.; Juliano, M. A.; Jansson, A. M. Azido acids in a novel method of solid-phase peptide synthesis. *Tetrahedron Lett.* **1997**, *38*, 2531−2534.
(22) Jost, M.; Greie, J. C.; Stemmer, N.; Wilking, S. D.; Altendorf, K.; Sewald, N. The first total synthesis of efrapeptin C. *Angew. Chem., Int. Ed.* **2002**, *41*, 4267−4269.
(23) Dal Pozzo, A.; Ni, M. H.; Muzi, L.; Caporale, A.; de Castiglione, R.; Kaptein, B.; Broxterman, Q. B.; Formaggio, F. Amino acid bromides: Their N-protection and use in the synthesis of peptides with extremely difficult sequences. *J. Org. Chem.* **2002**, *67*, 6372−6375.
(24) Bartra, M.; Romea, P.; Urpì, F.; Villarasa, J. A first procedure for the reduction of the azides and nitro compounds based on the reducing ability of $Sn(Sr)_3^-$ species. *Tetrahedron* **1990**, *46*, 587−594.
(25) Haubner, R.; Gratias, R.; Goodman, S. L.; Kessler, H. RGD plus X: Structure/Activity Investigations on Cyclic RGD-Peptides. *Peptides: Chemistry, Structure and Biology*; Kaumaya, P. T. P., Hodges, R. S., Eds.; Mayflower Scientific Ltd.: England, 1996; p 205.
(26) Ali, F. E.; Bennet, D. B.; Calvo, R. R.; Elliot, J. D.; Hwang, S. M.; Ku, T. W.; Lago, M. A.; Nichols, A. J.; Romoff, T. T.; Shah, D. H.; Vasko, J. A.; Wong, A. S.; Yellin, T. O.; Yuan, C. K.; Samanen, J. M. Conformationally constrained peptides and semipeptides derived from RGD as potent inhibitors of the platelet fibrinogen receptor and platelet aggregation. *J. Med. Chem.* **1994**, *37*, 769−790.
(27) Wermuth, J.; Goodman, S. L.; Jonczyk, A.; Kessler, H. Stereoisomerism and biological activity of the selective and superactive $\alpha_v\beta_3$ integrin inhibitor cyclo(RGDfV) and its retro-inverso peptide. *J. Am. Chem. Soc.* **1997**, *119*, 1328−1335.
(28) Dal Pozzo, A.; Fagnoni, M.; Bergonzi, R.; Vanini, L.; de Castiglione, R.; Aglio, C.; Colli, S. Synthesis and anti-aggregatory activity of linear retro-inverso RGD peptides. *J. Pept. Res.* **2000**, *55*, 447−454.
(29) Wüthrich, K. *NMR of Proteins and Nucleic Acids*; John Wiley: New York, 1986; p 186.

(30) Oishi, S.; Kamano, T.; Niida, A.; Odagaki, Y.; Hamanaka, N.; Yamamoto, M.; Ajito, K.; Tamamura, H.; Otaka, A.; Fujii, N. Diastereoselective synthesis of Ψ[(E)−CH═CMe]- and Ψ[(Z)−CH═CMe]-type alkene dipeptide isosteres by organocopper reagents and application to conformationally restricted cyclic RGD peptidomimetics. *J. Org. Chem.* **2002**, *67*, 6162−6173.
(31) Jäckel, C.; Koksch, B. Peptide design and protein engineering. *Eur. J. Org. Chem.* **2005**, 4483−4503.
(32) Bendall, J. G.; Payne, A. N.; Screen, T. E. O.; Holmes, A. B. Intrduction of bromine and chlorine substituents in medium ring ethers and lactones. *Chem. Commun.* **1997**, 1067−1068.
(33) Alper, P. B.; Hung, S. C.; Wong, C. H. Metal catalyzed diazo transfer for the synthesis of azides from amines. *Tetrahedron Lett.* **1996**, *34*, 6029−6032.
(34) Bax, A.; Davis, D. G. MLEV-17 based two-dimensional homonuclear magnetization transfer spectrscopy. *J. Magn. Reson.* **1985**, 355−360.
(35) Kumar, C. C.; Nie, H.; Rogers, C. P.; Malkowski, M.; Maxwell, E.; Catino, J. J.; Armstrong, J. Biochemical characterization of the binding of echistatin to integrin $\alpha_v\beta_3$ and $\alpha_v\beta_5$ receptor. *J. Pharmacol. Exp. Ther.* **1997**, *283*, 843−853.

JM0511334